ISSN: 0067-2904

Simulations of Four Types of Optical Aberrations using Zernik Polynomials

Uday E. Jallod
Department of Astronomy & Space, College of Science, University of Baghdad, Baghdad, Iraq.

Abstract

In this paper, a computer simulation is implemented to generate of an optical aberration by means of Zernike polynomials. Defocus, astigmatism, coma, and spherical Zernike aberrations were simulated in a subroutine using MATLAB function and applied as a phase error in the aperture function of an imaging system. The studying demonstrated that the Point Spread Function (*PSF*) and Modulation Transfer Function (*MTF*) have been affected by these optical aberrations. Areas under *MTF* for different radii of the aperture of imaging system have been computed to assess the quality and efficiency of optical imaging systems. Phase conjugation of these types aberration has been utilized in order to correct a distorted wavefront. The results showed that the largest effect on the *PSF* and *MTF* is due to the contribution of the third type coma aberrated wavefront.

Keywords: Aberration, Zernike polynomials, Fourier transform, and optical physics.

محاكاة أربعة أنواع للزيوغ البصرية باستخدام متعددة الحدود لزرنيك

عدي عطيوي جلود
قسم الفلك والفضاء، كلية العلوم، جامعة بغداد، بغداد، العراق.

الخلاصة

في هذا البحث، نفذت محاكاة حاسوبية لتوليد الزيغ البصري بواسطة متعددة الحدود لزرنيك. مثلت اربعة انواع مختلفة من الزيوغ لزرنيك باستخدام برنامج فرعي بلغة الماتلاب وطبقت كخطأ طور في فتحة النظام التصويري. بينت الدراسة ان دالة الانتشار النقطية ودالة التضمين الانتقالية تأثرت بهذه الزيوغ البصرية الاربعة. حسبت المساحات تحت دالة التضمين الانتقالية ولانصاف اقطار مختلفة لفتحة النظام التصويري لتقييم النوعية والكفاءة لانظمة التصوير البصرية. فرق الطور المرافق لهذه الزيوغ استخدم لتصحيح جبهة الموجة المشوهة. النتائج اظهرت انه اكبر تاثير على دالة الانتشار النقطية ودالة التضمين الانتقالية يعود الى جبهة الموجة المضطربة بمسهامة نوع الزيغ الثالث (coma).

Introduction

The optical quality of an optical imaging system is limited by wavefront diffraction and aberration. The aberrations are the main contributor to degradation into the observed wavefront lead to unwanted variations in the image intensity. Aberration is departure of the ideal wavefront within the exit pupil from its ideal form which is typically phase error [1]. An optical aberration is measured as the difference in optical path length between an aberrated and a reference wavefront. An unaberrated wavefront is converging and focusing to the Gaussian image point, but in the presence of aberration is causing a deviation from this focus [2]. In addition to the turbulence in the atmosphere, there are many sources of the phase error of the wavefront such as; optical misalignments, segmenting and phasing, and thermally induced distortions of optics [3].

Email: udayjallod@yahoo.co

There is a complex relationship between the phase aberration in the pupil function and the form of the focal spot. However, aberration leads to spreading of the focus both in the lateral plane, spatially an elongation along optical axis. This is accompanied by a reduction in the focal intensity. The distortion of the focal point reduces the resolution of the optical imaging system and cause blurring in an image plane [4]. There are a lot of studies of the aberration, but the two main methods are Karhunen – Loeve and Zernike polynomials [5]. The latter is studied in more details in this paper. The phase aberration is represented by normalized set orthogonal polynomials over on a unit circle, as Zernike polynomials. In 1953, Zernike won the Nobel Prize in physics for discovering the phase contrast technique. The advantage of Zernike polynomial is that the low order terms are related to the classical aberrations like astigmatism, coma and spherical aberrations [6].

The basic principal of conventional adaptive optics is to measure the aberration of an observed wavefront and apply compensating aberration in real time. Phase conjugation is the core of adaptive optics, and it could be analyzed in different methods. The most important way is the field of a distorted wavefront by its complex conjugate [7].

In this paper, the mathematical equations that compute Zernike polynomials have been studied and simulated in order to demonstrate the essential features for four types of aberrations. The normalized Point Spread Function (*PSF*) and Modulation Transfer Function (*MTF*) are computedin order to assess the quality imaging system in the presence of the aberrations. Areas under *MTF* have been calculated to illustrate the ability of the imaging system to resolve the astronomical objects in the presence of aberration. The correction of the aberration is applied by phase conjugation.

Basic Theory:

The pupil function that incorporates the complete information about imaging properties of any an optical system is presented by [8]:

$$P(\eta,\gamma) = A(\eta,\gamma)\exp[\phi(\eta,\gamma)] \tag{1}$$

where $A(\eta,\gamma)$ is a circular aperture representing the pupil with a normalized amplitude transmittance, (η,γ) are the spatial variables and $\phi(\eta,\gamma)$ is the phase of the pupil function.

The pupil function in the absence of an aberration is determined from [9]:

$$P(\eta,\gamma) = \begin{cases} 1 & \text{inside } A(\eta,\gamma) \\ 0 & \text{otherwise} \end{cases} \tag{2}$$

The phase error associated with the aperture of an optical imaging system consisting of Zernike polynomials. There are several definitions of Zernike polynomial [10- 12]:

$$Z_n^m(\rho,\theta) = \sqrt{2(n+1)}R_n^m(\rho)G^m(\theta) \tag{3}$$

where *m* and *n* are non – negative integers, and $m \le n$, ρ,θ are polar coordinates. However, it is convenient to write $Z_n^m(\rho,\theta)$ with just one index.

$$Z_i = \begin{cases} \sqrt{2(n+1)}R_n^m(\rho)G^m(\theta) & \text{m} \neq 0 \\ R_n^0(\rho) & \text{m} = 0 \end{cases} \tag{4}$$

where *i* is the mapping of (*n*, *m*). The radial and azimuthal factors $R_n^m(\rho)$ and $G^m(\theta)$ are given by:

$$R_n^m(\rho) = \sum_{s=0}^{(n-m)/2} \frac{(-1)^s (n-s)!}{s!(\frac{n+m}{2}-s)!(\frac{n-m}{2}-s)!} r^{n-2s} \tag{5}$$

$$G^m(\theta) = \begin{cases} \sin(m\theta) & \text{i odd} \\ \cos(\text{m}\theta) & \text{i even} \end{cases} \tag{6}$$

The resolution at the image plane is determined by the width of the *PSF*. *PSF* for an imaging system is proportional to the modulus square of the Fourier transform of its pupil function and could be written as [13]:

$$PSF(x,y)=\left|\int_{-\infty}^{\infty}\int_{-\infty}^{\infty}P(\eta,\gamma)e^{-2i\pi(u\eta+v\gamma)}d\eta d\gamma\right|^2 \tag{7}$$

Another property that evaluates the quality of an image forming is the *MTF*. *MTF* of an imaging system describe how the sharpness and the contrast of an object are captured in the resulting image because *MTF* could reflect the characteristics spatial frequency response of an imaging system [14]. *MTF* could be written as:

$$MTF(u,v)=\left|\Im(PSF(x,y))\right| \tag{8}$$

where $\Im$ is the Fourier transform.

The fundamental equation to be used for the formation of an image by an optical imaging system is given by [15]:

$$G(x,y)=\int_{-\infty}^{\infty}\int_{-\infty}^{\infty}O(\eta,\gamma)PSF(x-\eta,y-\gamma)d\eta d\gamma \tag{9}$$

where $G(x,y)$ is the observed or recorded image intensity, $O(x,y)$ is the object intensity, $PSF(x,y)$ is the blurring image caused by an optical imaging system.

The above equation could also be written as [16]:

$$G(x,y)=O(x,y)\otimes PSF(x,y) \tag{10}$$

These two equations are representing a convolution equation, and $\otimes$ denotes convolution operator.

Simulations and Results:

A circular function has been simulated in an array of size 128 by 128 which has unity magnitude of radius equal to (20) pixels, according to the following equation [17]:

$$A(\eta,\gamma)=\begin{cases}1 & \text{if } \sqrt{(\eta-\eta_c)^2+(\gamma-\gamma_c)^2}\le 20\\ 0 & \text{otherwise}\end{cases} \tag{11}$$

where (η_c, γ_c) is the center of the two – dimensional array. In the case of a transparent pupil with aberration, $P(\eta,\gamma)$ represents the aberration function.

The phase across the aperture is expanded in term of Zernike polynomial. Zernike polynomial is defined in polar coordinates, $\eta=\rho\sin(\theta)$ and $\gamma=\rho\cos(\theta)$, i.e. optical phase given in eq. (1) equal to Zernike polynomial which given in eq. (4) as given by [18]:

$$P(\eta,\gamma)=A(\eta,\gamma)e^{z_i(\eta,\gamma)} \tag{12}$$

There are more than thirty seven kinds of Zernike polynomials, but four types of Zernike aberrations have been studied in this paper. These are defocus, astigmatism, coma and spherical which have the values of (*n*, *m*) as follow (2, 0), (4, 2), (5, 1), and (6, 0) respectively. These types are chosen because they represent the most commonly used types of aberrations.

The equations (3 – 6) that evaluate Zernike aberrations have been used and a called in subroutine by MATLAB function. It should be noted that the factorial in eq. (5) are coded in MATLAB as gamma function $[s!=\Gamma(s+1)]$ because the gamma function is much faster than the factorial function.

Figure-1 illustrates the four different types of Zernike polynomials.

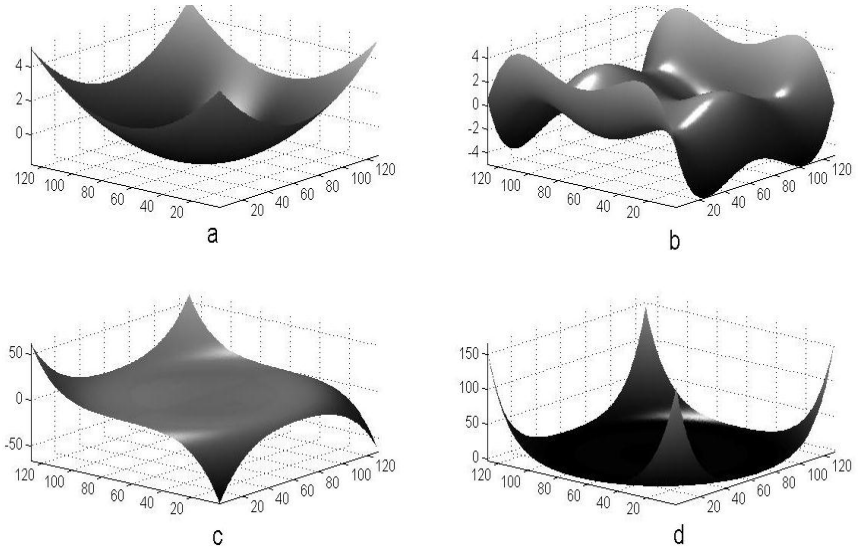

Figure 1 – (a) Defocus aberration, (b) Astigmatism aberration, (c) Coma aberration, (d) Spherical aberration.

In this study, the observed wave is considered as a plane wave, which means that there is no effect from the atmospheric turbulence on it. Therefore, the wavefront is transmitted through the pupil function according to eq. (12) is distorted as shown in Figure-2.

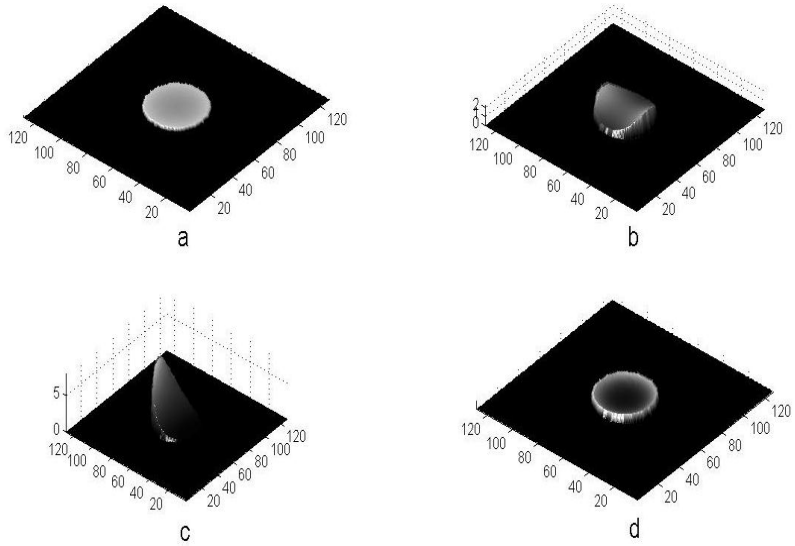

Figure 2 – The aberrated wavefront at exit pupil by; (a) The defocus aberration, (b) The astigmatism aberration, (c) The coma aberration, (d) The spherical aberration.

The *PSF* has been simulated by taking the fast Fourier transform of the pupil function that associated with the optical phase error in term of Zernike polynomial. Figure-3 demonstrates the *PSF* for the kinds of aberrations that have been studied in this paper.

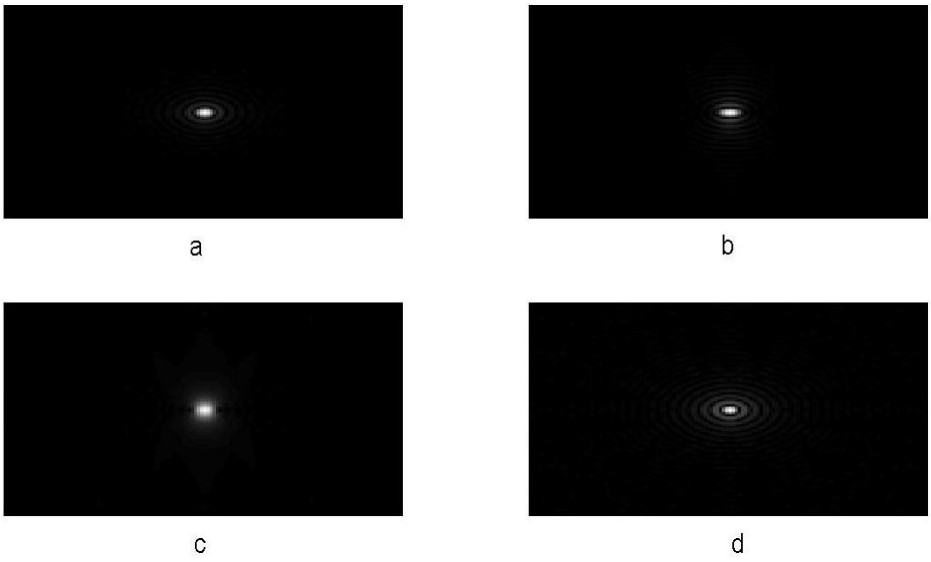

Figure 3 – The *PSF* of the aberrated wavefront for (a) The defocus aberration, (b) The astigmatism aberration, (c) The coma aberration, (d) The spherical aberration.

In addition to *PSF*, the *MTF* has been computed using eq. (8) in order to study the effect of aberrations on an optical system. Figure-4 shows the *MTF* of the four types of aberrations investigated in this work.

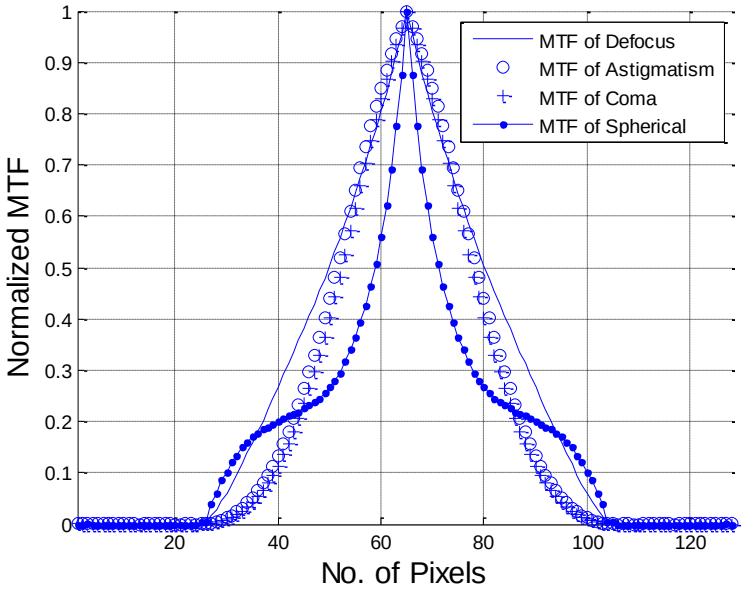

Figure 4 – Normalized *MTF* for different types of aberrations.

In this study, the area under the normalized *MTF* is also computed using the following finite integral:

$$Area = \int_{1}^{N}\int_{1}^{N} MTF(x,y)dxdy = \sum_{1}^{N}\sum_{1}^{N} MTF(x,y) \quad (13)$$

where N=128, and step size of summation is equal to one pixel.

Area under *MTF* is plotted as a function of different radii of the aperture. These radii have been taken from (10 – 50) pixels correlated with the size of the array as shown in the Figure-5.

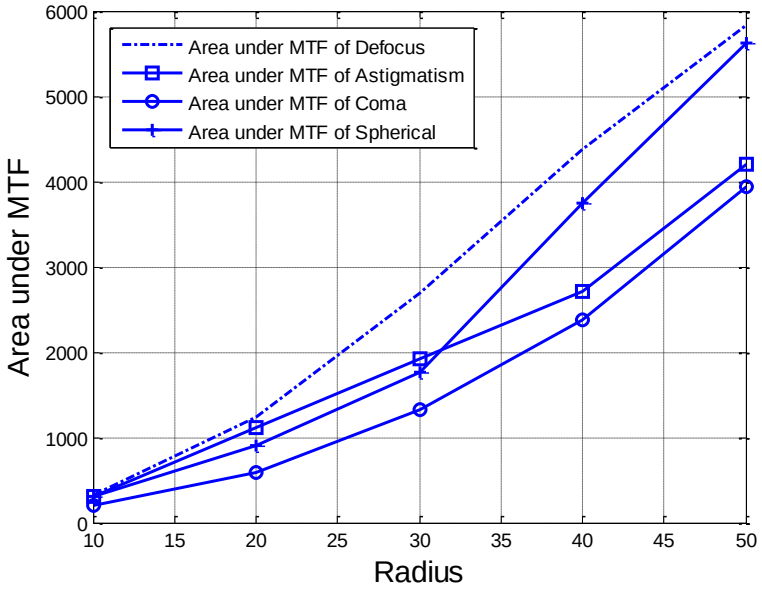

Figure 5 – Area under *MTF* for four different types of aberrations at different radii.

In order to expand our simulations, a binary system is considered as an original object and displayed in Figure-6 (a). This binary is generated diagonally and separated by a distance of 10 pixels from the center of the array and have the same magnitude. It should be pointed out here that the binary system is simulated at the same size of the pupil function (128 × 128), and could be written as [19]:

$$B(\eta,\gamma)=\begin{cases}1 & \text{at } (\eta_c,\gamma_c)\,\&\,(\eta_c+10,\gamma_c+10)\\ 0 & \text{eleswhere}\end{cases} \tag{14}$$

The Fourier transform is applied to compute the fringes of the binary system (see Fig.(6 – b)).

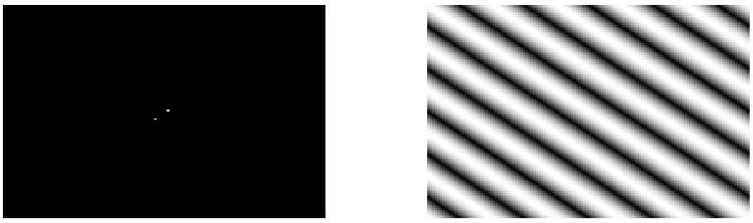

a b

Figure 6- (a) Simulation a binary system as a reference of an object, (b) Fringes of the binary system.

The observed images of this binary system observed by an optical telescope with these types of aberrations are simulated according to eq. (10), and shown in Figure-7.

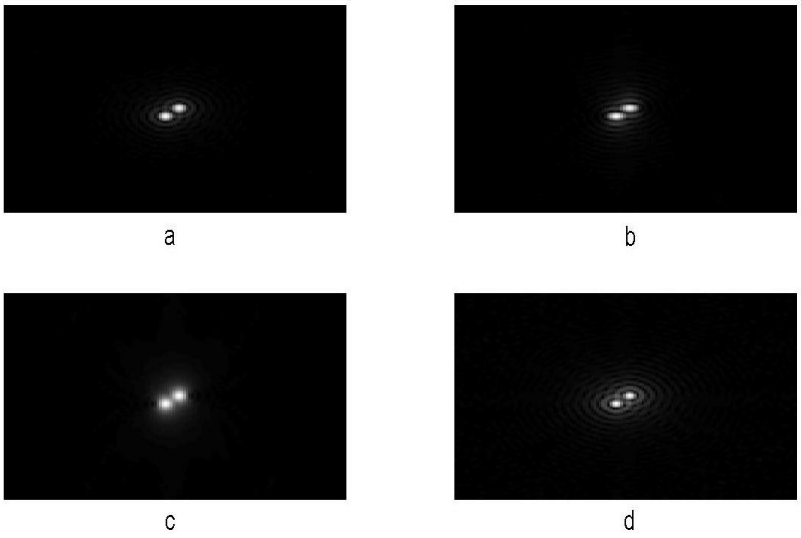

Figure 7 – The observed image of a binary system observed by an optical imaging system; (a) The defocus aberration, (b) The astigmatism aberration, (c) The coma aberration, (d) The spherical aberration.

The phase conjugation is considered to be one of the applications of adaptive optics which can be used to correct the optical phase error. The phase conjugation could be computed by multiplying the phase error by its complex phase conjugate. Therefore, the pupil function could be written in term phase conjugation as [20]:

$$P(\eta,\gamma) = A(\eta,\gamma)e^{z_i(\eta,\gamma)}e^{-z_i(\eta,\gamma)} \quad (15)$$

where $z_i(\eta,\gamma)$ is the phase error.

The results after the correction using above equation are demonstrated in Figure-8.

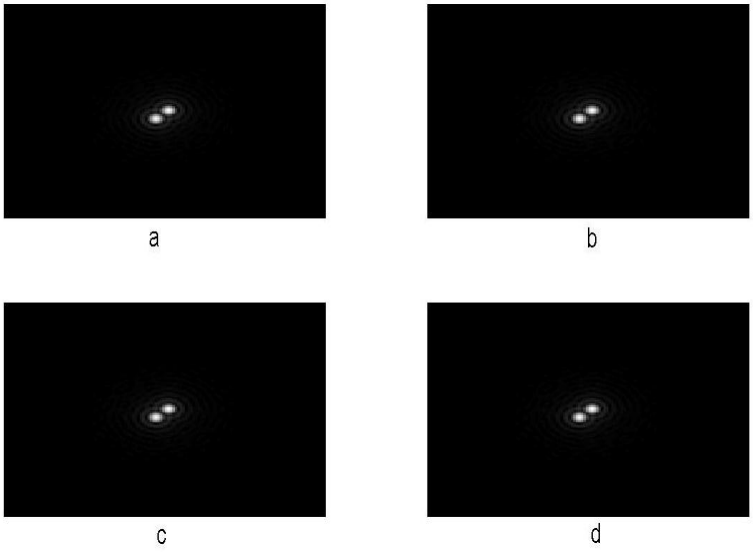

Figure 8 – The observed image of the same binary observed with phase conjugate; (a) The defocus aberration, (b) The astigmatism aberration, (c) The coma aberration, (d) The spherical aberration.

The magnitude of correction is the difference between the corrected and the uncorrected images of the binary system (i.e. Figure-7 & Figure- 8), therefore, the subtraction between them has been applied and could be written as:

$$Gs = |Ga - Gc| \quad (16)$$

where *Ga* is the image of the binary system with aberration, and *Gc* is the same image with correction. The absolute value is taken just for displaying in order to neglect the negative values as shown in Figure-9.

Figure 9 – The correction magnitude is used by phase conjugate of; (a) The defocus aberration, (b) The astigmatism aberration, (c) The coma aberration, (d) The spherical aberration.

The maximum value of correction magnitude is computed of each type aberration and could be written as:

$$Gs_{\max} = Max(Max(Gs)) \quad (17)$$

This value demonstrates the lowest and the highest effect of the aberrations on the optical imaging system.

MTF after correction using phase conjugation becomes coincided at same position of four types aberrations as shown Figure-10.

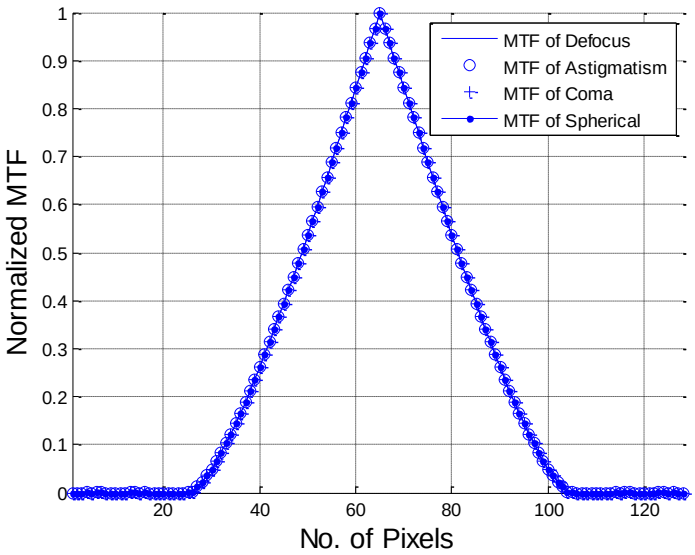

Figure 10 – Normalized *MTF* of four different types of aberrations.

Conclusions

Several important points could be concluded from this work:-

1. The *MTF* of the coma aberration is a vital type that affect on the image plane as shown in Figure-4.

2. The lowest area under *MTF* is for the coma aberration which means that this type covers less information about observed object than others as shown in Figure-5.
3. Phase conjugate technique has been utilized to reduce the effect of aberration, but as shown in Figure-8, there is no free phase error because the limited size of the pupil function which has been used in our simulation.
4. The values of $Gs_{\max}$ was computed using eq. (17) demonstrated that the defocus, astigmatism, coma, and spherical have the values (0.0248, 0.1294, 0.3282, and 0.1321) respectively. These values indicate that the lowest effect on the imaging system is due to the contribution of the defocus aberration, while the highest effect comes from the coma type.

References

1. Remon, L., Ferrando,V., Ruis, L. M, Ballester, E., Furlan, W. D.and Monsorui, J.A. **2015**. Computational Fourier Optics Simulation using a Virtual Laboratory. 43rd Annual Conference SEFI, France, 29 June – 2 July.
2. Brummelaar T. A. **1996**. Modeling Atmospheric Wave Aberrations and Astronomical Instrumentation using the Polynomials of Zernike. *Optics Communication Journal*, **132**: 329 – 342.
3. Ersoy, O. **2007**. *Diffraction, Fourier Optics and Imaging*. John Wiley & Sons, Canada. pp: 173.
4. Nathan, D. **2000**. Image Sharpening Metrics and Searching Strategies for Indirect Adaptive Optics. Ph. D Thesis, university of Durham, U.K. pp: 26.
5. Watson, A. B. **2015**. Computing Human Point Spread Functions. *Journal of Vision*, **15**(2): 1- 25.
6. Saha, S. **2007**. *Diffraction – limited Imaging with Large and Moderate Telescopes*. World Scientific Publishing Co., Singapore. pp: 264-268.
7. Plainis, P. Pallikeres, I.G. **2008**. Ocular Monochromatic Aberration Statistics in a Large Emmetropic Population. *Journal of Modern Optics*, **55**(4 – 5): 759 – 772.
8. Arnison, M. **2003**. Phase Contrast and Measurement in a Digital Microscopy, Ph. D. Thesis, School of Physics, University of Sydney, pp. 70.
9. Neil, M., Booth, M. and Wilson, T. **2000**. Closed - Loop aberration Correction by use of a Model Zernike Wave – Front Sensor, *Journal of Optics Letters*, **25**(15): 1083 – 1085.
10. Booth, M. **2007**. Adaptive Optics in Microscopy. *Journal of the Philosophical Transaction Royal Society*, **365:** 2829 – 2843.
11. Shmidt, J.D. **2010**. *Numerical of Optical Wave Propagation with Examples in MATLAB*. Society of Photo – Optical Instrumentation Engineers (SPIE), pp: 66 – 69.
12. Marray, L. P. **2006**. Smart Optics: Wavefront Sensor – Less Adaptive Optics – Image Correction through Sharpness Maximization. Ph.D. Thesis. Galway, University of Ireland, pp: 17 – 24.
13. Mohammed, A.T. **2007**. Limits of the Efficiency of Imaging with Obstructing Apertures. *SQU: Sultan Qaboos University Journal for Science*, **12**(1), pp: 67-74.
14. Estaban, D., Sosa, S. and T,oro, L. **2011**. Understanding the Physical Optics Phenomena by using a Digital Application for Light Propagation. *Journal of Physics*, **274**: 1- 12.
15. Mohammed, A.T. and Jallod, E. Uday. **2013**. Numerical Simulations of Imaging Extrasolar Planets using Circular and Square Apodized Apertures. *J. Baghdad for Sci*., **10**(4): 1232-1241.
16. Goodman, J. W. **2000**. *Statistical Optics*. John Willy & Sons.Inc, New York. pp: 169-171.
17. Maurer, L. **2013**. Simulating Interference and Diffraction in Instructional Laboratories. *Physical Education Journal*, **48**(2), pp: 227 – 232.
18. Jallod, U.E. **2015**. Simulation of Fraunhofer Diffraction for Plane Wave using Different Apertures. *Iraqi Journal of Science*, **56**(2A): 1198 – 1207.
19. Hassan, Fouad N. **2011**. Imaging Binary Stars in the Presence of Defocusing. *Iraqi Journal of Science*, **52**(4): 519 – 524.
20. Tyson, R. K. **2011**. *Principal of Adaptive Optics*. Third Edition, Taylor and Francis Group, USA. pp: 55 – 57.